Research paper

MEF2C repressor variant deregulation leads to cell cycle re-entry and development of heart failure

Ana Helena M. Pereira[a,1], Alisson C. Cardoso[a,1], Silvio R. Consonni[b], Renata R. Oliveira[a], Angela Saito[a], Maria Luisa B. Vaggione[a], Jose R. Matos-Souza[c], Marcelo F. Carazzolle[d], Anderson Gonçalves[a], Juliano L. Fernandes[e], Gustavo C.A. Ribeiro[f], Mauricio M. Lopes[g], Jeffery D. Molkentin[h], Kleber G. Franchini[a,c,*]

[a] Brazilian Biosciences National Laboratory (LNBio), Brazilian Center for Research in Energy and Materials (CNPEM), 13083-970 Campinas, Sao Paulo, Brazil
[b] Department of Biochemistry and Tissue Biology, University of Campinas, Campinas, Brazil
[c] Department of Internal Medicine, University of Campinas, Campinas, Brazil
[d] Genomics and Expression Laboratory, University of Campinas, Campinas, Brazil
[e] Jose Michel Kalaf Research Institute, Campinas, Brazil
[f] Cardiovascular Surgery, Pontifical Catholic University, Campinas, Brazil
[g] Cardiology, Pontifical Catholic University, Campinas, Brazil
[h] Cincinnati Children's Hospital Medical Center, University of Cincinnati, Cincinnati, USA

ARTICLE INFO

ABSTRACT

Background: A pathophysiological link exists between dysregulation of MEF2C transcription factors and heart failure (HF), but the underlying mechanisms remain elusive. Alternative splicing of MEF2C exons α, β and γ provides transcript diversity with gene activation or repression functionalities.

Methods: Neonatal and adult rat ventricular myocytes were used to overexpress MEF2C splicing variants $\gamma+$ (repressor) or $\gamma-$, or the inactive *MEF2Cγ+23/24* (K23T/R24L). Phenotypic alterations in cardiomyocytes were determined by confocal and electron microscopy, flow cytometry and DNA microarray. We used transgenic mice with cardiac-specific overexpression of MEF2Cγ+ or MEF2Cγ− to explore the impact of MEF2C variants in cardiac phenotype. Samples of non-infarcted areas of the left ventricle from patients and mouse model of myocardial infarction were used to detect the expression of MEF2Cγ+ in failing hearts.

Findings: We demonstrate a previously unrealized upregulation of the transrepressor MEF2Cγ+ isoform in human and mouse failing hearts. We show that adenovirus-mediated overexpression of MEF2Cγ+ downregulates multiple MEF2-target genes, and drives incomplete cell-cycle reentry, partial dedifferentiation and apoptosis in the neonatal and adult rat. None of these changes was observed in cardiomyocytes overexpressing MEF2Cγ−. Transgenic mice overexpressing MEF2Cγ+, but not the MEF2Cγ−, developed dilated cardiomyopathy, correlated to cell-cycle reentry and apoptosis of cardiomyocytes.

Interpretation: Our results provide a mechanistic link between MEF2Cγ+ and deleterious abnormalities in cardiomyocytes, supporting the notion that splicing dysregulation in MEF2C towards the selection of the MEF2Cγ+ variant contributes to the pathogenesis of HF by promoting cardiomyocyte dropout.

Funding: São Paulo Research Foundation (FAPESP); Brazilian National Research Council (CNPq).

1. Introduction

Heart failure (HF) is a prevalent and morbid illness caused by many common diseases such as ischaemic heart disease, hypertension and diabetes. Typically, the onset of HF is gradual and arises from the progressive adverse remodelling of the cardiac chambers and the decline in pumping function [1]. Although many potentially unfavourable alterations may contribute to the remodelling process and progression to HF, the dropout of cardiomyocytes, related either to their degeneration or death, is a central component to the

* Corresponding author at: Brazilian Biosciences National Laboratory (LNBio), Brazilian Center for Research in Energy and Materials (CNPEM), 13083-970 Campinas, Sao Paulo, Brazil.
E-mail address: kleber.franchini@lnbio.cnpem.br (K.G. Franchini).
[1] Both authors contributed equally to this manuscript.

Research in Context section

Evidence before this study

Heart failure (HF) remains a significant cause of disability and mortality worldwide. At the cellular level, HF correlates to pathological changes in cardiomyocytes driven by dysregulated signal transduction cascades, which in turn alters downstream transcriptional programs. Previous studies indicate an essential role of the *Myocyte Enhancer Factor 2C* (*MEF2C*) transcriptional regulator in the HF, but the underlying mechanisms were unclear. Interestingly, alternative splicing of MEF2C exons α, β and γ provides transcript diversity with gene activation or repression functionalities, imposed by the alternative expression of the γ exon. In this study, we explored the hypothesis that the selective expression of the transrepressor MEF2Cγ+ variant may be a critical determinant of the detrimental cardiac effects of MEF2C.

Added value of this study

We identified the transrepressor variant MEF2Cγ+ as a detrimental factor or mediator in HF. Our findings show that MEF2Cγ+ is significantly upregulated in human and murine failing hearts. Overexpression of MEF2Cγ+ either in cardiomyocytes or in cardiac-specific transgenic mice induces an overall downregulation of genes related to sarcomere, cytoskeleton and energy metabolism, while genes related to cell cycle were upregulated. Accordingly, differentiated cardiomyocytes overexpressing the transrepressor MEF2Cγ+ re-entered into the cell cycle but did not execute cytokinesis. These events culminate in multinucleation and apoptosis, accelerating the vicious cycle in the pathophysiology of HF.

Implications of all the available evidence

We suggest that enhanced expression of MEF2Cγ+ is maladaptive and maybe a critical factor in the pathogenesis of HF. In this regard, inhibiting the splicing reactions that favour the appearance of the repressor variant of MEF2C might potentially constitute a new therapeutic modality to interfering in the progression of HF.

performance declining in failing hearts [2,3]. Both degeneration and death are outcomes of the pathological responses of cardiomyocytes to long-term exposure to neurohormonal and mechanical stressors that occur in the settings of the HF predisposing diseases and risk factors [4]. The cellular processes leading to these events denote an extensive transcriptional reprogramming of cardiac gene expression, which results in altered expression of genes encoding components of the sarcomere, cytoskeleton, calcium handling, ion transport and energy metabolism [5]. Preclinical and clinical studies have defined a small set of transcription factors (e.g. MEF2 and NFAT) that are drivers of the unfavourable transcriptional reprogramming and the maladaptive remodelling in failing hearts [5,6]. It remains unclear, however, how the dysregulation of transcription factors contributes to the dropout of cardiomyocytes in failing hearts.

Research in cardiac models has provided evidence for essential roles of the *Myocyte Enhancer Factor 2* (*MEF2)* family of transcriptional regulators (encoded by four genes: *Mef2a, -b, -c,* and *-d*) in the pathological cardiac remodelling and failure. Forced expression of MEF2A, MEF2C or MEF2D in the postnatal mouse heart translates into pathological remodelling, featured, with some differences of detail, by dilated cardiomyopathy with little or no hypertrophy [7–9]. In contrast, inhibition of MEF2 signalling by a dominant-negative MEF2

mutant protein in the mouse adult heart attenuates the development of cardiomyopathy triggered by the calcineurin activation [7]. Moreover, depletion of *Mef2c* by siRNA attenuates both the hypertrophic cardiac growth and the upregulation of *Natriuretic Peptide A* (NPPA) in response to pressure overload [10]. Consistent with the observations in mouse models, human genetic studies have shown alterations in the expression of genes regulated by MEF2 in patients in the end stage of HF [11]. Furthermore, increased expression of MEF2C in the left ventricle has been reported as a hallmark of human HF [12]. Less is known, however, regarding the molecular and cellular processes underlying the deleterious influence of MEF2 in the heart.

Regulation of the MEF2 function is reported to occur by various means, including the control of MEF2 protein abundance, post-translational modifications and association with other transcription factors and co-regulators [13]. Also, *Mef2* genes use alternative splicing to encode transcripts with three possible differentially regulated spliced exons [14,15]. At least eight different splice variants of MEF2C are predicted, according to the composition of the alternative expression of the exon 3 (either $\alpha 1$ or $\alpha 2$), the inclusion/exclusion of the β domain and the inclusion/exclusion of the γ fragment from the last coding exon [15]. The mutually exclusive splicing exons $\alpha 1$ and $\alpha 2$, which encode the 3′ region adjacent to the MADS/MEF2 DNA binding domain, has been reported to be directly regulated by the splicing factor Rbfox1 [16]. Notably, *Rbfox1* repression correlates to an enhanced $\alpha 1/\alpha 2$ ratio and the development of cardiac hypertrophy and HF in the mouse. The β exon encodes a domain that contains multiple acidic residues in the cognate proteins. The insertion of this domain in the MEF2 protein substantially enhances the activity of the transactivation domain; however, only the transcripts expressed in the brain and in skeletal muscles seem to contain this domain [15]. The domain encoded by the last coding exon of MEF2 genes is fully included in all MEF2A and MEF2D variants. However, in the transcripts of MEF2C, an alternative splicing process may yield the inclusion or exclusion of the γ fragment (32 amino acid residues) of the last domain. Intriguingly, the inclusion of the γ fragment in the MEF2C transcripts entails a transrepressor functionality that is dependent on the phosphorylation of the Ser396 residue within this fragment in the cognate protein [15]. *Mef2c* is expressed predominantly as γ− isoforms in the healthy mouse heart [14]; however, the implications of the γ fragment inclusion in the MEF2C for the homeostasis of the heart remain unexplored.

In this study, we have characterized the biological role and potential clinical relevance of the MEF2Cγ+ transrepressor variant in the pathogenesis of HF. Specifically, we demonstrate that the levels of MEF2Cγ+ are increased in the failing mouse and human hearts. Our results highlight that upregulation of MEF2Cγ+ promotes an extensive transcriptional reprogramming accompanied by a partial cell cycle re-entry, dedifferentiation and apoptosis of cardiomyocytes, thereby contributing to the adverse remodelling of the failing hearts. These results provide a new understanding of MEF2C implications for HF, where MEF2Cγ+ upregulation causes a previously unappreciated transcriptional reprogramming associated with pathological cardiac remodelling.

2. Materials and methods

2.1. Animals

Primary cultures of neonatal (NRVMs) and adult rat ventricular myocytes (ARVMs) were obtained from 1 to 2 day-old and 6 to 8 week-old Wistar rats, respectively. Male mice 10−12 week-old were used to generate myocardial infarction through left coronary artery ligation. We purchased the transgenic mice FVB-Tg(Myh6-Mef2c) from The Jackson Laboratory (Bar harbor Maine, USA), stock number 010586. The MEF2Cγ- transgenic mice were generated by the Model Organism Laboratory at LNBio/CNPEM, as detailed in the Supplementary Material. The transgenic mice used in this study were males

aged 4 to 6 months. All animals were handled in compliance with the principles of laboratory animal care formulated by the Animal Care and Use Committee of the State University of Campinas protocol number 3095-1 and Animal Care and Use Committee CEUA/CNPEM protocol number 12 and 31.

2.2. Human studies

The study has been carried out following the Declaration of Helsinki (2000) of the World Medical Association and has been approved by the Pontifical Catholic University of Campinas, Institutional Ethics Committee. All patients gave informed consent.

2.3. Patient selection

Patients with myocardial infarction, left ventricle (LV) dysfunction and with akinetic wall region determined by cardiac magnetic resonance imaging (MRI) were selected for LV reconstruction and revascularization. The decision regarding revascularization was based on clinical grounds (symptoms, presence/absence of ischemia/viability, and angiographic findings) [17].

2.4. Operative procedure

With the patient supported by cardiopulmonary bypass, myocardial protection was achieved with antegrade and retrograde blood cardioplegia. The ventricular restoration was performed using the technique described previously as endoventricular reconstruction [18].

2.5. Tissue sampling

Endomyocardial biopsy samples were taken from the LV remote area previously selected according to cardiac MRI. The samples were immediately frozen in liquid nitrogen and stored at $-80\ °C$.

2.6. Quantification of mRNAs

The total RNA from cardiac or cell samples was isolated using Trizol® according to the manufacturer's instructions. For mRNA quantification, target genes expression was analysed by SYBR Green qPCR (with Dissociation Curve) program on the Mx3000TM Comparative Quantitative PCR System (Stratagene). The oligonucleotides used in this study were listed in Supplementary Table 1. All reactions were performed with reference dye normalisation. The median cycle threshold value was used for analysis, and all cycle threshold values were normalised to the GAPDH mRNA expression level.

2.7. Total RNA from human hearts

The amounts of the MEF2C transcripts in the samples of the left ventricle of patients with myocardial infarction were compared with those in commercially available total RNA from Normal Human Heart Left Ventricle (BioChain Institute Incorporated, Newark, CA, catalog number: R1234138-50), as described by the manufacturer.

2.8. Confocal microscopy

Fixed tissue sections and cells were blocked with 1% BSA, 0.1% Triton-X, 50 nM Glycine in 0.1 M PBS on ice. The samples were incubated with phospho-histone H3 ser10 − pH3 antibody (06−570, Millipore) overnight at 4 °C. Alexa Fluor-488-conjugated goat anti-rabbit (1:200) or Alexa Fluor-568-conjugated goat anti-mouse (1:200) secondary antibodies were used at room temperature. Alternatively, samples were incubated with rhodamine-conjugated phalloidin (1:50; Molecular Probes) at room temperature for two h. The slides were then mounted with VectaShield with DAPI. Samples were examined using a Leica TCS SP8 confocal on a Leica DMI 6000.

2.9. Transmission electron microscopy

For cell samples, the culture medium was replaced by a fixative solution consisting of 2.5% glutaraldehyde, sodium cacodylate buffer (0.1 M) at pH 7.4 and $CaCl_2$ (3 mM) for 5 min at room temperature and additional 1 h on ice. The cells were then rinsed with cacodylate buffer/$CaCl_2$ and were post-fixed in 1% OsO_4, cacodylate buffer (0.1 M), $CaCl_2$ (3 mM), and potassium ferrocyanide solution (0,8%) for 30 min on ice. Next, the cells were washed with Milli-Q water and stained with uranyl acetate (2%) overnight at 4 °C. The cells were then washed in milli-Q water and dehydrated in an ethanol gradient. Then, adherent cells were embedded in Epon 812 resin. Resin polymerization was controlled in an incubator (60 °C) for 72 h. Monolayer culture ultra-thin sections were stained with uranyl acetate and lead citrate. For heart samples, small pieces were fixed in 2.5% glutaraldehyde (Electron Microscope Science, Hatfield, PA, USA) in 0.1 M cacodylate buffer containing 0.3% tannic acid for 4 h at 4 °C. After, the tissues were post-fixed with 1% osmium in 0.1 M cacodylate buffer for 1 h and then dehydrated through a graded series of acetone and embedded in Epon (EMbed-812; Electron Microscopy Sciences, Hatfield, PA). Ultrathin sections were stained with uranyl acetate and lead citrate. The sections were examined using an LEO 906 (Zeiss) electron microscope operated at 60 kV. For the quantification of the fragmented sarcomeres, digital electron microscopy pictures of each group of the study were taken randomly at a magnification of 12,930x and 16,700x. A total of 20 fields of view per group were used to analyze more than 300 sarcomeres. The percentage of fragmented sarcomere was annotated.

2.10. Data sharing

The microarray data files (Affymetrix CEL files) for all the experiments described here have been deposited to GEO under the superseries GSE99748.

2.11. Statistical analyses

Data were presented as mean± standard error of the mean (SEM) and analysed by ANOVA with Bonferroni multiple comparisons test for *posthoc* comparisons or by Student's *t*-test. No statistical methods were used to predetermine the sample size. Statistical significance of categorical values between groups was designated $p < 0.05$.

3. Results

3.1. MEF2Cγ repressor variant is increased in human and mouse HF

To gain insight into the relevance of MEF2C in the pathophysiology of HF we sought to examine the expression of the transcripts of the MEF2C and the splicing variant domains α, β and γ (Fig. 1a), in healthy versus failing human hearts. We used samples of commercially available total RNA derived from healthy human left ventricles ($n = 5$) as controls and biopsy samples of non-infarcted remote zone obtained from the left ventricle of patients ($n = 14$) with chronic ischemic cardiomyopathy. Clinical and cardiac magnetic resonance imaging (MRI) characteristics of the study group are reported in Supplementary Table 2. The abundance of full-length *MEF2C* was increased in most samples of failing hearts (Fig. 1b). Neither the α1 nor the α2 domain-containing MEF2C transcripts were altered in the RNA samples of failing as compared to those of healthy hearts (Supplementary Figure 1a−c). The β domain was detected neither in the healthy nor in the failing hearts. Notably, however, the
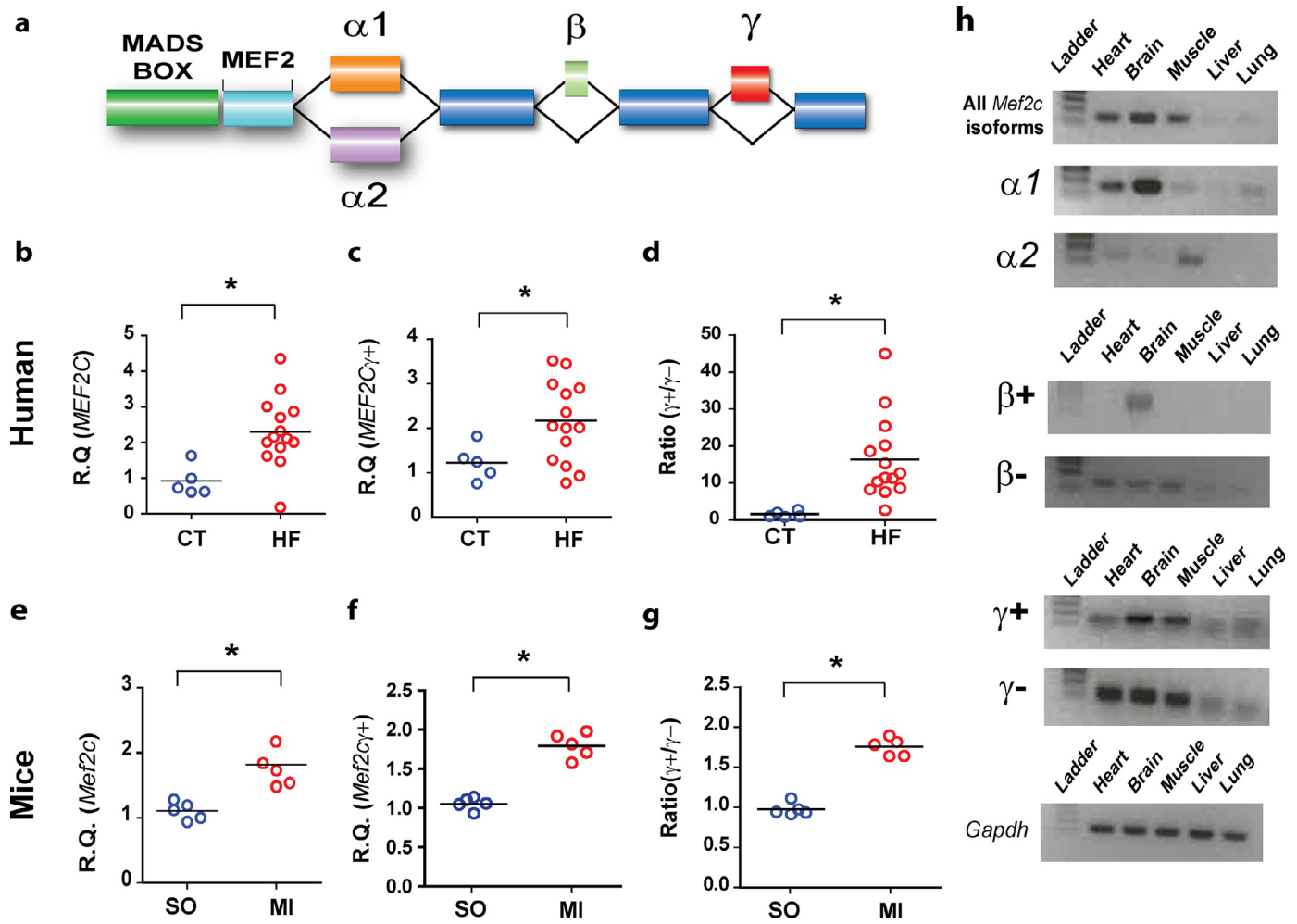
Fig. 1. Expression of MEF2Cγ+ repressor variant in normal and failing hearts. (a) Schematic representation of the MEF2C gene and alternative exons, including the mutually exclusive exons α1 & α2, the skipping exon β, and 3′splice site selection of γ domain; (b) Real time PCR of *MEF2C* in normal and failing human hearts. (CT *N* = 5; HF *N* = 14); (c) Real time PCR of *MEF2Cγ+* variant in normal and failing human hearts. (CT *N* = 5; HF *N* = 14); (d) *MEF2Cγ+/ MEF2Cγ-* expression ratio in normal and failing human hearts. (CT *N* = 5; HF *N* = 14); (e) Real time PCR of *Mef2c* in sham operated and myocardial infarction mouse model. (*N* = 5); (f) Real time PCR of *MEF2Cγ+* repressor variant in sham operated and myocardial infarction mouse model. (*N* = 5); (g) *MEF2Cγ+/ MEF2Cγ-* expression ratio in sham operated and myocardial infarction mouse model. (*N* = 5); (h) RT-PCR assay showing the expression of alternative exons *α*, *β* and *γ* of *Mef2c* in healthy wild type mouse tissues. Real time data are presented as mean ±s.e.m. Unpaired Student *t-test* (*$p < 0.05$ vs CT). R.Q.: Relative Quantification.

expression of *MEF2C* transcripts containing the γ fragment (γ+) was significantly increased, while those lacking the γ fragment (γ-) were decreased in samples of failing as compared to those of healthy human hearts, resulting in a substantial increase of the γ+/γ− ratio in the failing hearts (Fig. 1c and d). Therefore, we conclude that there is an increased expression of MEF2C in failing human hearts, which relies on the enhanced expression of the variants containing the γ fragment.

Next, we examined the content of the transcripts of the full-length MEF2C and the *α*, *β* and *γ* domains in the remote zone of the left ventricle from infarcted and sham-operated mice. The abundance of full-length *MEF2C* was increased in most samples of failing hearts (Fig. 1e). The transcripts containing the α1 and α2 domains were similarly expressed (Supplementary Figure 1d−f), while the transcripts containing the β domain were not detected in samples of the healthy or failing mouse hearts. Consistent with the data obtained in the failing human hearts, the content of the γ+ fragment was significantly increased in the hearts from infarcted as compared to those of sham-operated mice (Fig. 1f and g).

We also examined the expression of the *α*, *β* and *γ* domains of MEF2C by RT-PCR in different mouse tissues (heart, brain, skeletal muscle, liver and lung). We observed abundant expression of MEF2C

in the brain followed by the heart and the skeletal muscle, with negligible expression in the liver and the lung (Fig. 1h). The transcripts containing α1 domain expressed predominantly in the brain and the heart, while the transcripts containing α2 domain predominates in the skeletal muscle. The β domain was expressed in the brain tissue, with negligible expression in other tissues. The transcripts containing the γ fragment were preferentially detected in the brain, skeletal muscle and heart, respectively, but the predominance in these tissues was of transcripts lacking the γ fragment. Overall, our present observations cast *MEF2C γ+/γ−* ratio, as a potential marker of failing heart, prompting us to investigate the effects of overexpression of the MEF2γ- and the MEF2γ+ isoforms in cardiomyocytes.

3.2. MEF2Cγ+ overexpression promotes sarcomeric disassembly and apoptosis in cardiomyocytes

We transduced NRVMs with adenoviral expression vectors to address the effects of MEF2Cγ+, MEF2Cγ− and the MEF2Cγ+23/24 (K23T/R24L) a transcriptionally inactive mutant resulting from loss or diminished DNA binding, on the phenotype and survival of cardiomyocytes. The transductions of the expression vectors were all efficient, as indicated by the comparable expression levels of each type
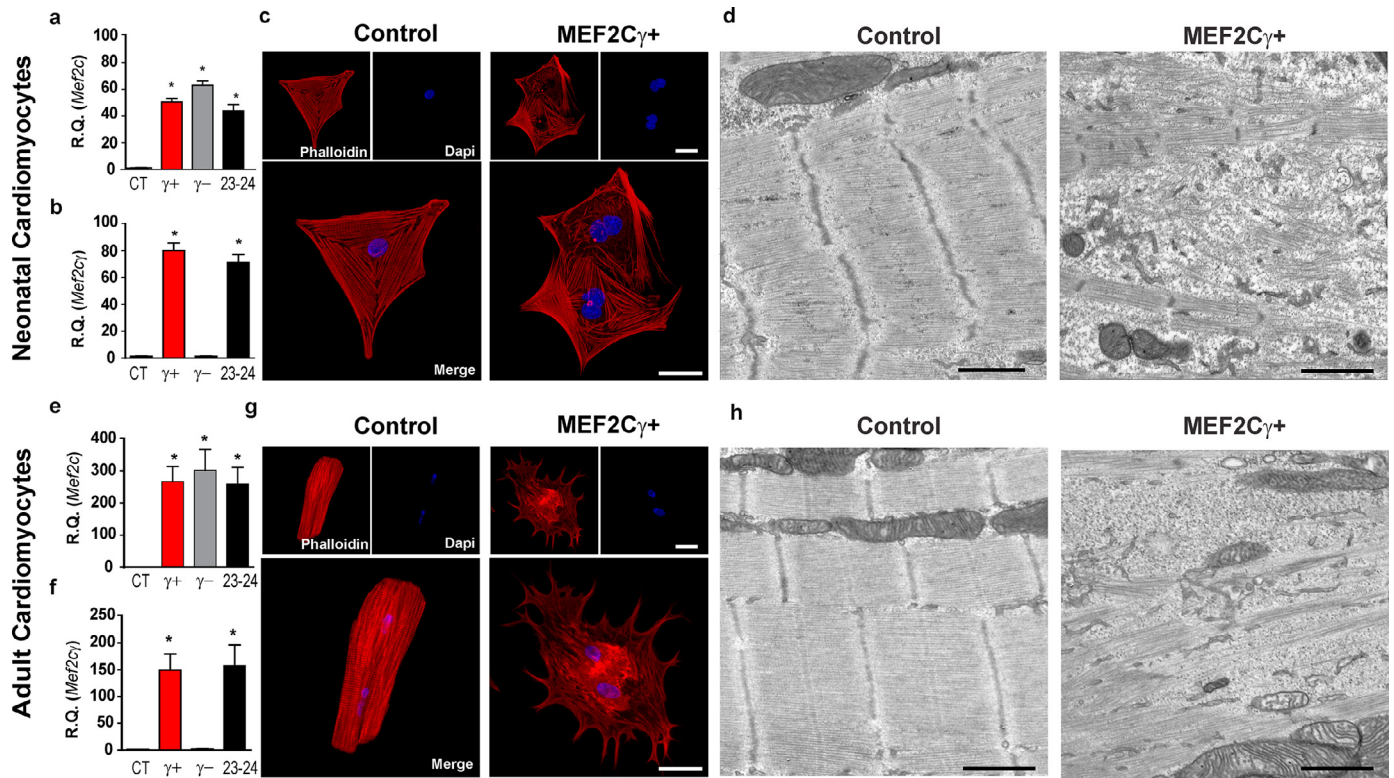
Fig. 2. MEF2Cγ+ overexpression promotes sarcomere disarray and multinucleation of cardiomyocytes in vitro. (a) Real time PCR of MEF2C transcripts in samples of neonatal rat ventricular myocytes (NRVMs) controls (CT) or transduced with adenovirus carrying MEF2Cγ+, MEF2Cγ- or the mutant MEF2Cγ+23/24 isoform genes, as indicated. (N = 6); (b) Real time PCR of MEF2 γ repressor domain in NRVMs control or transduced with adenovirus particles, as indicated. (N = 6); (c) Confocal maximum-intensity z-projections of CT or transduced MEF2Cγ+ NRVMs stained with rhodamine-conjugated phalloidin (red) and DAPI (blue). The MEF2Cγ+ overexpression induces loss and disassembles of sarcomeric filaments and promotes multinucleation in NRVMs. Merged images are composed of phalloidin and DAPI. Scale bar: 20 μm. (N = 3); (d) Transmission electron micrographs of CT or NRVMs transduced with MEF2Cγ+, showing that the MEF2Cγ+ overexpression induces loss of sarcomeric integrity and disrupts the Z-line organization. Scale bar: 1 μm (N = 3); (e) Real time PCR of Mef2c gene in adult cardiomyocytes control (CT) or transduced with adenovirus carrying MEF2Cγ+, MEF2Cγ- or MEF2Cγ+23/24 isoform genes, as indicated. (N = 6); (f) Real time PCR of MEF2C γ repressor domain in adult cardiomyocytes, as indicated. (N = 6); (g) Confocal maximum-intensity z-projections of CT or transduced MEF2Cγ+ adult cardiomyocytes stained rhodamine-conjugated phalloidin (red) and DAPI (blue). The transduced myocytes showed a rounded appearance with only a myofibrilar core remaining. Scale bar: 20 μm. (N = 3); (h) Transmission electron micrographs of CT or transduced MEF2Cγ+ in adult cardiomyocyte. Note that the MEF2Cγ+ induces gradual loss of sarcomeric myofilaments and disrupts the sarcomeric organization. Scale bar: 1 μm. (N = 3); Real time data are presented as mean ±s.e.m. One-way ANOVA. (*p < 0.05 vs CT). (For interpretation of the references to color in this figure legend, the reader is referred to the web version of this article.)

of MEF2C transcript in the NRVMs (Fig. 2a). The expression levels of the transcripts containing the γ fragment in cardiomyocytes transduced with similar amounts of the MEF2Cγ+, MEF2Cγ− and MEF2Cγ+23/24 adenoviral vectors are shown in Fig. 2b.

The expression of the recombinant MEF2Cγ+ (48 h) caused striking morphological changes in the NRVMs. Confocal microscopy observation showed pronounced depletion and disarray of sarcomeres in the perinuclear area (Fig. 2c). Also, we observed an increased number of large and bizarre shape nuclei of cardiomyocytes overexpressing MEF2Cγ+ (Fig. 2c and Supplementary Figure 2b). Notably, no significant morphological change was found in the cardiomyocytes overexpressing MEF2Cγ− or MEF2Cγ+23/24 (Supplementary Figure 2c). At the ultrastructural level, cells overexpressing MEF2Cγ+ showed extensive sarcomeric disassembly and areas containing remnants of the sarcomeres such as clumped Z-band material (Fig. 2d). No such alterations were seen in NRVMs overexpressing MEF2Cγ− or the inactive MEF2Cγ+23/24 (Supplementary Figure 2d).

We used TUNEL imaging assay to determine whether the overexpression of MEF2Cγ+, MEF2Cγ− or MEF2Cγ+23/24 might affect NRVMs viability. We found an increase in the number of TUNEL-positive NRVMs (2-fold) after the transduction with the MEF2Cγ+ vector, as compared to the cells transduced with MEF2Cγ− or MEF2Cγ+23/24 vectors (Supplementary Figure 3a and b). To further explore the impact of the MEF2Cγ+ in NRVMs viability, we extended the observation period to five days after the transduction with the viral vector. Distinct from the control

cells, most of the cardiomyocytes transduced with MEF2Cγ+ showed morphological features of apoptosis (Supplementary Figure 3c).

Because there may be differences in the responses between cardiomyocytes derived from neonatal and adult rat hearts to the overexpression of MEF2Cγ+, we next examined if the results observed in the NRVMs could be reproduced in cardiomyocytes isolated from adult rats (ARVMs). We used ARVMs cultured for 48 h after the transduction with adenoviral vectors MEF2Cγ+, MEF2Cγ− or MEF2Cγ+23/24. The efficiency of the transductions in the ARVMs was equivalent among the adenoviral vectors (Fig. 2e). The transcripts containing the γ fragment increased in the cells transduced with the MEF2Cγ+ vector and in those transduced with the MEF2Cγ+23/24 vector (Fig. 2f). The morphology of the ARVMs at 48 h after the transduction with the viral vectors showed control cardiomyocytes with the characteristic rod shape and preserved sarcomeric structure (Fig. 2g). In contrast, the majority of the ARVMs transduced with the MEF2Cγ+ vector lost their rod shape and showed disorganization of the sarcomeric structure (Fig. 2g). The sarcoplasm of the ARVMs transduced with the MEF2Cγ+ vector spread all over the culture dish surface, filled with phalloidin positive material, likely Actin stress fibre; remnants of the sarcomeric structure of the myofibrils were still present at the centre of the cells. Despite the lack of changes in the number of nuclei, we did see consistent increases in the nuclear area of the ARVMs transduced with MEF2Cγ+ vector (Supplementary Figure 3d). ARVMs transduced with MEF2Cγ−, or MEF2Cγ+23/24 vectors were morphologically similar to the control cells

(Supplementary Figure 3e). At the ultrastructural level, ARVMs transduced with the MEF2Cγ+ vector showed depletion of sarcomeric structure, particularly in the cell periphery (Fig. 2h). No significant change was observed at the ultrastructural level in the ARVMs transduced with MEF2Cγ−, or MEF2Cγ+23/24 vectors, as compared to control cells (Supplementary Figure 3f). These are the first data to characterize the cardiomyocyte alterations induced by MEF2Cγ+ and reveal that this repressor variant of MEF2C may lead to sarcomeric disassembly and changes in the cell nuclei that culminate in cell death.

3.3. Transcriptomic differences in cardiomyocytes overexpressing MEF2C variants

Next, we used cDNA microarrays to profile gene expression and compare the relative abundance of gene transcripts in the NRVMs overexpressing the MEF2C variants (MEF2Cγ+, MEF2Cγ− or MEF2Cγ+23/24) as compared to control cells. We used total RNA extracted from cells 48 h after the viral vector transduction. Statistical analysis was performed with the aim of identifying genes that were differentially expressed between the groups, by a criterion of at least a 2.0-fold change and an adjusted value of $P < 0.05$ (Deposit number GSE99748, GEO database). Overexpression of MEF2Cγ+ resulted in a significant difference in NRVMs transcripts, with 1250 transcripts differentially expressed (676 upregulated and 574 downregulated) out of a total of 28,827, relative to control cardiomyocytes (Supplementary Figure 4a and d). Remarkably, neither MEF2Cγ− nor MEF2Cγ+23/24 induced substantial changes in gene expression as compared to control cardiomyocytes (Supplementary Figure 4b and c; e and f). As expected, Mef2c transcripts were enriched in NRVMs transduced with MEF2Cγ+, MEF2Cγ− or MEF2Cγ+23/24 vectors (Supplementary Figure 4a−c). At an initial analysis, we paid particular attention to genes that are known to be targets of MEF2, as annotated in the Ingenuity knowledge-based pathway analysis. Alterations in the expression of the transcripts from 28 MEF2 target genes emerged in the NRVMs overexpressing MEF2Cγ+, including genes encoding muscle-specific structural, cytoskeletal, metabolic, stress-responsive proteins and transcription factors (Supplementary Table 3). Notably, all these MEF2 target genes were found to be downregulated in the cardiomyocytes overexpressing MEF2Cγ+.

Previous studies have shown that the transrepression function of the gamma domain acts autonomous, i.e., does not involve cis effects on other MEF2 protein functions outside of the domain. However, it remains unclear whether the transrepressor variant interferes in the transactivation function of MEF2 signalling. Here, to test this premise, COS cells were cotransfected with the 3x-MEF2 reporter gene and constructs encoding MEF2A, MEF2D, MEF2Cγ- and MEF2Cγ+. We found that MEF2Cγ+ functioned as a dominant-negative form by inhibiting the transcriptional activity of MEF2A, MEF2Cγ- and MEF2D (Supplementary Figure 2a). These data agree with the repressive effect of the MEF2Cγ+ variant on the gene programs under control by MEF2 transcription factors.

3.4. Defining MEF2Cγ+ -associated pathways

In further analysis, genes differentially expressed in NRVMs transduced with MEF2Cγ+ were clustered by function using Gene Ontology (GO) to enrich biological pathways (Fig. 3a). Supplementary Table 4 provides the complete list and p-values of differentially expressed transcripts and the top associated biological pathways. Transcripts differentially expressed in NRVMs transduced with MEF2Cγ+ vector clustered in three main cellular and molecular processes classifications: (i) cell cycle, (ii) energy metabolism, and (iii) cellular component organization. Approximately 10% (124) of the transcripts differentially expressed were annotated as regulators of the cell cycle. A large subset of these transcripts (n = 110) was upregulated in NRVMs transduced with the

MEF2Cγ+ vector. The top-ranked genes of this subset were selected for confirmation by real-time PCR, including Cyclin E1 (Ccne1), Cyclin-dependent Kinase 2 (Cdk2) and Aurora Kinase B (Aurkb). Transcripts of all three genes were confirmed to be significantly upregulated in the cardiomyocytes overexpressing MEF2Cγ+ (Fig. 3b−d). Approximately 29% (365) of the differentially expressed transcripts were classed into the clusters of metabolic processes, of which 182 were reduced in cells transduced with the MEF2Cγ+ vector. Several of these genes are predicted to encode proteins related to energy metabolism (Supplementary Table 4). Reductions in the transcripts of muscle creatine kinase (Ckm), peroxisome proliferator-activated receptor alpha (Ppara), PPARG coactivator 1 alpha (Ppargc1a) and PPARG coactivator 1 beta (Ppargc1b) were confirmed by RT-PCR (Fig. 3e−h). Approximately 3% [35] of the differentially expressed transcripts were classed into the clusters of cellular organization and structure, with a subset downregulated, including sarcomeric genes, such as Sarcomeric α-actinin (Actn2), Cardiac Actin (Actc1), Desmin (Des) and Myosin Heavy Chain isoform α (Myh6) (Fig. 3i−l). Notably, no significant change was observed in the gene expression profile of cardiomyocytes transduced with MEF2Cγ− or MEF2Cγ+23/24, as compared to control cardiomyocytes. Several of the genes related to cell cycle, cell metabolism and cellular organization and structure were also changed in adult cardiomyocytes transduced with MEF2Cγ+ (Supplementary Figure 4 g−o). These results support a role for MEF2Cγ+ in downregulating gene programs related to metabolism, cell organization and structure, but intriguingly, in upregulating markers of cell cycle program in differentiated cardiomyocytes.

3.5. MEF2Cγ+ stimulates NRVMs cell cycling

Next, we investigated if MEF2Cγ+ could change cell cycle activity in cardiomyocytes. Initially, we performed a detailed analysis of the DNA content of NRVMs by propidium iodide flow cytometry. We observed an accumulation of cells in G2/M phase 48 h after the transduction with the MEF2Cγ+ expression vector (Fig. 4a). Transduction with the MEF2Cγ+ vector increased the amount of NRVMs in G2/M to 58 ± 2%, while transduction with the MEF2Cγ− (22 ± 2%) or MEF2Cγ+23/24 (21 ± 1%) did not change the amount of NRVMs in the G2/M, as compared to controls (22 ± 2%), indicating that overexpression of MEF2Cγ+ might stimulate cell cycle re-entry in NRVMs.

DNA-synthesis and cell cycle re-entry does not necessarily result in mitosis and cytokinesis in cardiomyocytes. Thus, we performed immunofluorescence staining using an antibody directed to the histone H3 phosphorylated at Ser-10 (pH3), a marker of mitotic activity [19,20]. Transduction of NRVMs with MEF2Cγ+ vector increased the number of pH3 positive cardiomyocytes, by 3-fold, as compared to control and to cells transduced with the MEF2Cγ−, or the MEF2Cγ+23/24 vectors (Fig. 4b). Next, we directly assessed the number of binucleated and multinucleated cardiomyocytes overexpressing MEF2Cγ+. Comparisons with NRVMs transduced with MEF2Cγ−, or MEF2Cγ+23/24 vectors revealed a MEF2Cγ+-dependent increase of binucleated and multinucleated cardiomyocytes by approximately 3-fold (Supplementary Figure 2b). These findings indicate that MEF2Cγ+ enhances the DNA synthesis in NRVMs but not the progress through cytokinesis.

3.6. Repression of cyclin-dependent kinase inhibitors parallel MEF2Cγ+ induced cardiomyocyte cycling

We then raised the question as to whether the ability of MEF2Cγ+ to determine the cell cycle re-entry in NRVMs might be related to reductions in the abundance of Cyclin-dependent Kinase (CDK) inhibitors, which are critical regulators of cell cycle progression. To date, previous studies have shown that Cdkn1a (P21) is a MEF2-responsive gene [21]. Moreover, our microarray data indicated that the transcripts of Cdkn2b (p15) were reduced in cells transduced with the MEF2Cγ+ vector. We then monitored the expression patterns of the transcripts of
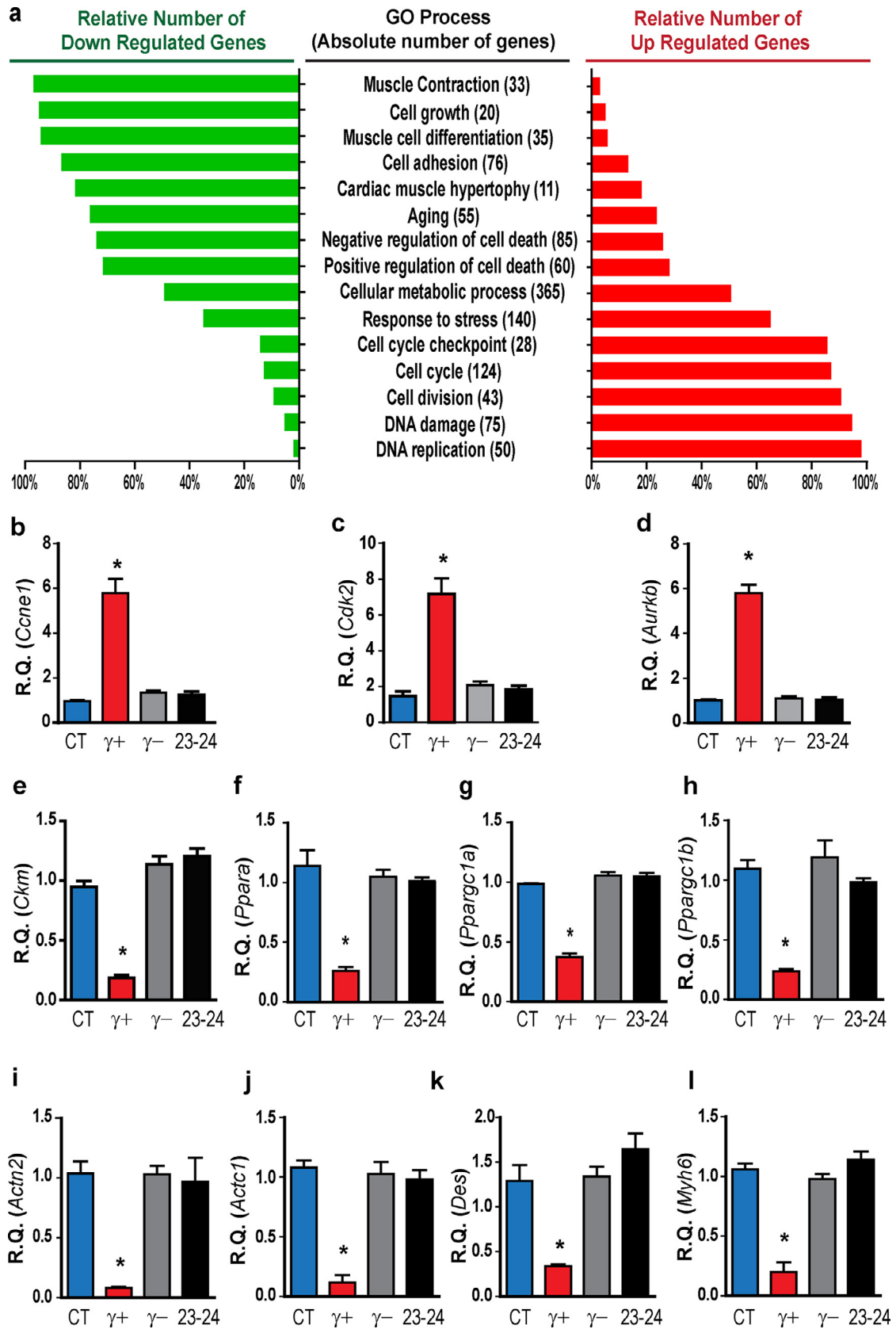
Fig. 3. Transcriptome profiling of cardiomyocytes overexpressing MEF2Cγ+. (a) Absolute and relative number of genes involved in each biological process clustered by function as biological description in Gene Ontology (GO) process. See Supplementary Table 4 for *p-value* and gene list included in each process; (b-l) Validation of microarray targets and analysis of gene expression of cell cycle, metabolism and structural candidate genes by quantitative real time PCR in samples of control (CT) NRVMs or transduced with adenovirus carrying MEF2Cγ+, MEF2Cγ- or mutant MEF2Cγ+23/24 isoform genes, as indicated. (N = 6). Real time data are presented as mean ±s.e.m. One-way ANOVA (*$p < 0.05$ vs CT).
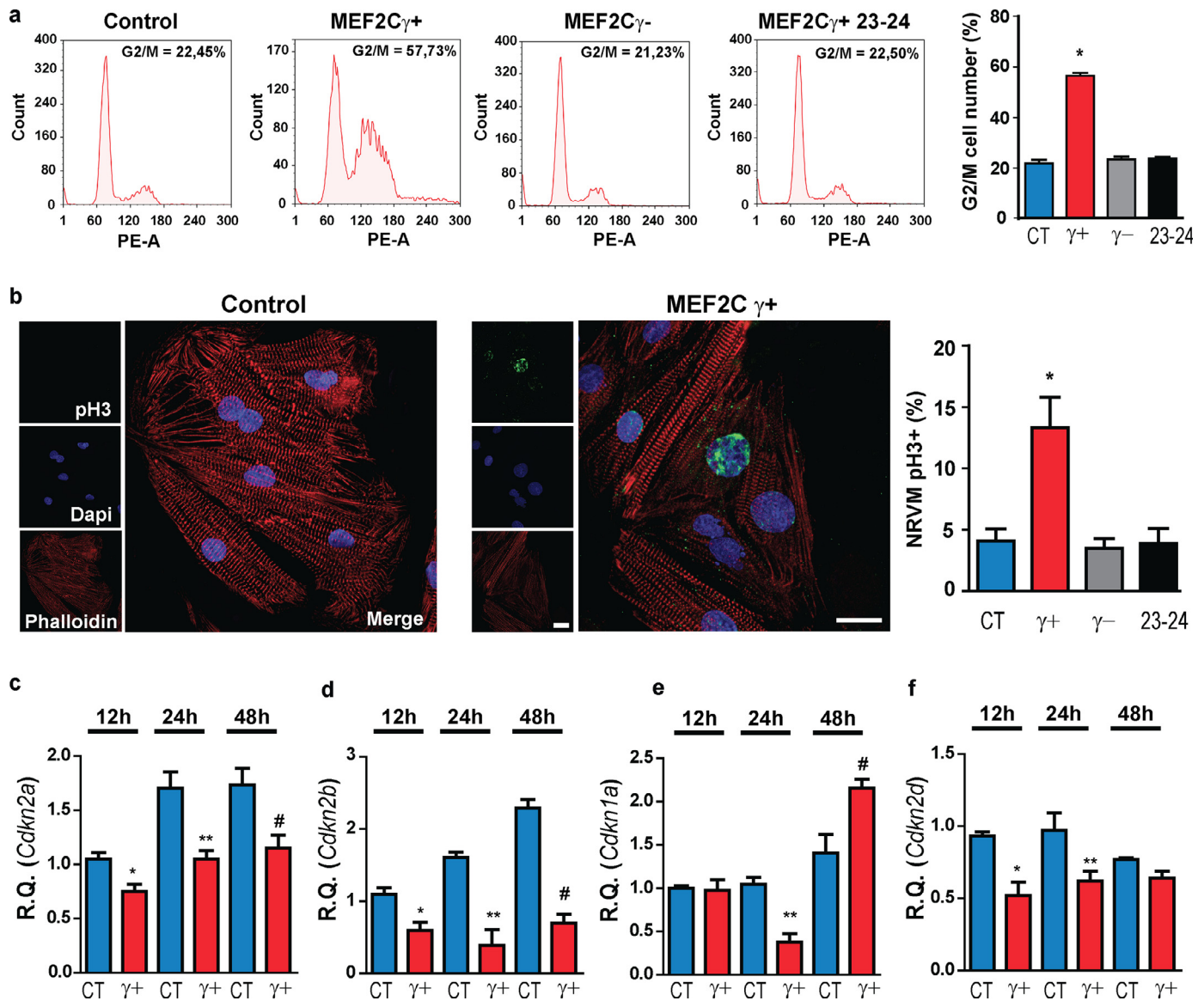
Fig. 4. MEF2Cγ+ overexpression stimulates cell cycle reentry in NRVMs. (a) Diagrams and bar graph quantification of propidium iodide flow cytometry in control (CT) NRVMs or transduced with adenovirus particles carrying MEF2Cγ+, MEF2Cγ- or MEF2Cγ+23/24 isoform genes, as indicated.(N = 9) Data are presented as mean ±s.e.m. One-way ANOVA (*p < 0.05 vs CT); (b) Confocal maximum-intensity z-projections of control or MEF2Cγ+ adenovirus transduced NRVMs stained with anti-pH3 (green), DAPI (blue) and rhodamine-conjugated phalloidin (red). Scale bar: 20 μm. Graph quantification of the percentage (%) of pH3 positive NRVMs. (N = 5) Data are presented as mean ±s.e.m. (*p < 0.05 vs CT); (c–f) Real time PCR of CDK inhibitors genes, CDKN2A (p16), CDKN2B (p15), CDKN1A (p21), CDKN2D (p19) in samples of NRVMs control (CT) or transduced with adenovirus particles carrying MEF2Cγ+, MEF2Cγ- or MEF2Cγ+23/24 isoform genes, for 12, 24 or 48 h (N = 6). Data are presented as mean ±s.e.m. One-way ANOVA (*p < 0.05 vs CT12h, **p < 0.05 vs CT24h, #p < 0.05 vs CT48h).

CDK inhibitors in NRVMs through a period ranging from 12 to 48 h after the transduction with the MEF2Cγ+ vector. Cdkn2a (p16) and Cdkn2b (p15) were both significantly reduced in NRVMs throughout the 48 h after the transduction with the MEF2Cγ+ vector in comparison to control cells (Fig. 4c and d). Cdkn1a (p21) and Cdkn2d (p19) were both significantly reduced in cells 24 h after the transduction with MEF2Cγ+ vector, but not after that (Fig. 4e and f). Thus, these results suggest that MEF2Cγ+ induced cell cycle re-entry in differentiated cardiomyocytes might result from downregulation of cell cycle inhibitors.

3.7. MEF2Cγ+ but not MEF2Cγ− transgenic mice display dilated cardiomyopathy

Previous work has provided compelling evidence that transgenic MEF2C heart-restricted overexpression leads to dilated cardiomyopathy and heart failure in mice [8]. However, those studies did not clearly define as to which MEF2C variant (MEF2Cγ+ or MEF2Cγ-) was

expressed in the transgenic mice. Here, we performed targeted transgene sequencing and real-time PCR analysis to demonstrate that the MEF2C transgenic mice overexpressed, in fact, MEF2Cγ+. Thus, to address the role of the γ fragment of MEF2C in the cardiac homostasis, we used the previously published transgenic line that overexpresses the variants α1/β−/γ+ (TgMEF2Cγ+) [8] and produced a new transgenic line, which overexpresses α1/β−/γ− (TgMEF2Cγ−). The MEF2Cγ+ and MEF2Cγ− mRNA levels were examined by qPCR, and the transcripts were shown to be increased by 13 and 17 folds, respectively (Supplementary Figure 5a and b). Echocardiography analyses indicated a moderate systolic dysfunction of the LV only in the TgMEF2Cγ+ (Supplementary Table 5). At necropsy, TgMEF2Cγ+ transgenic mice exhibited enlarged ventricular chambers, as compared to TgMEF2Cγ− and control mice (Fig. 5a). Cardiac histological changes in TgMEF2Cγ+ mice included a reduction in the diameter of cardiomyocytes but no significant interstitial fibrosis (Supplementary Figure 5c and d). Electron microscopy analysis of the hearts from the TgMEF2Cγ

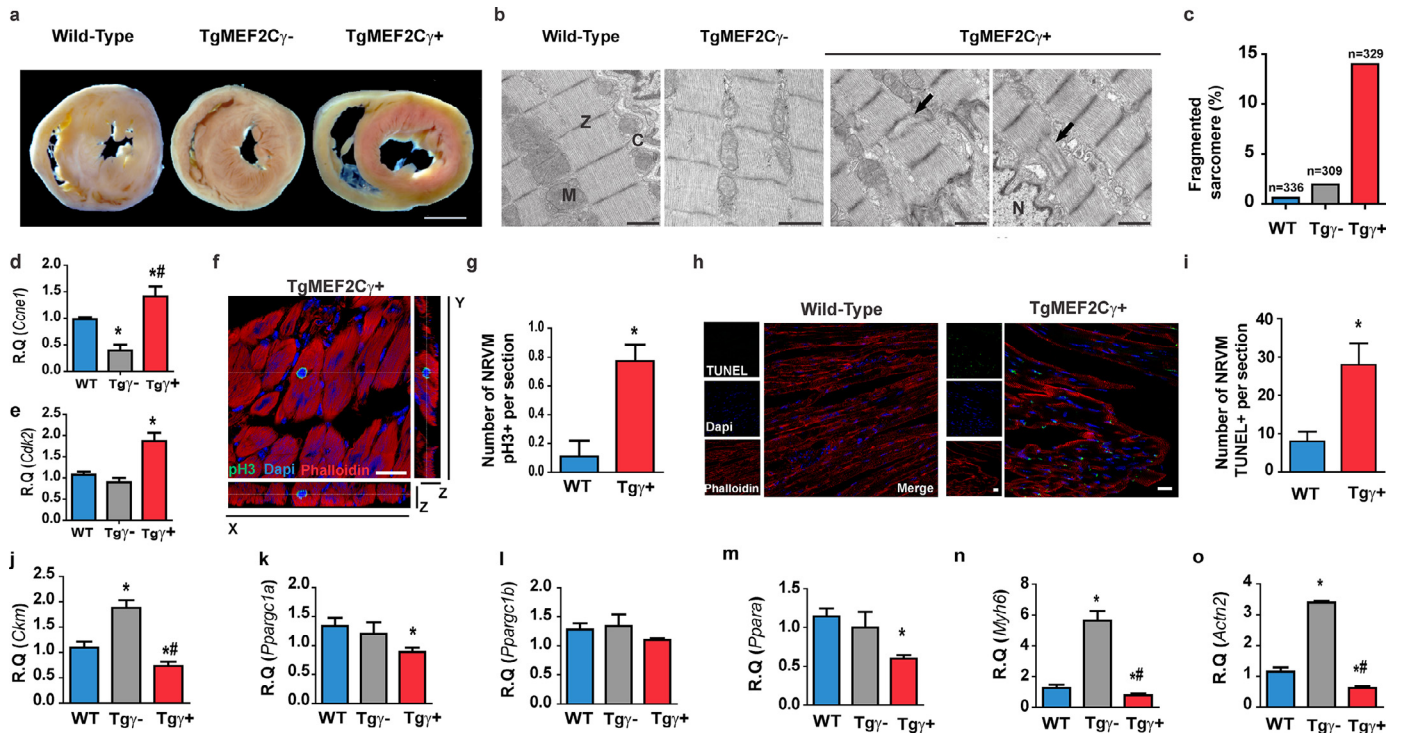**Fig. 5.** Dilated cardiomyopathy in MEF2Cγ+ transgenic mice. (a) Representative picture of transverse sections of WT, TgMEF2Cγ- and TgMEF2Cγ+ mice hearts. Scale bar: 4.5 mm; (b) Transmission electron micrographs of WT, TgMEF2Cγ- and TgMEF2Cγ+ mice showing several fragmented sarcomeres (arrows) in the TgMEF2Cγ+. Z: z-disc; C: costameres; M: mitochondria. Scale bar: 1 μm (N = 3); (c) Graph quantification of the percentage of fragmented sarcomere by transmission electron micrograph analysis of WT, TgMEF2Cγ- and TgMEF2Cγ+ mice. The total number of analysed sarcomeres is displayed above each bar; (d and e) Real-time PCR of cell cycle genes of WT, TgMEF2Cγ- and TgMEF2Cγ+ mice hearts. (N = 6); (f) Z-stack confocal microscopy of TgMEF2Cγ+ heart section stained with anti-phosphohistone H3 Ser10 (pH3) (green), DAPI (blue) and rhodamine-conjugated phalloidin (red). Scale bar: 20 μm; (g) Graph quantification of the number of pH3 positive cardiomyocytes per sections in WT and TgMEF2Cγ+. (N = 3); (h) TUNEL assay performed in sections from WT and TgMEF2Cγ+ hearts. Scale bar: 20 μm; (i) Graph quantification of the number of TUNEL positive cardiomyocytes per section in WT and MEF2Cγ+ mice. (N = 3); (j−m) Real-time PCR of metabolism genes in heart from WT, TgMEF2Cγ- and TgMEF2Cγ+ mice. (N = 6); (n and o) Real-time PCR of structural genes in heart from WT, TgMEF2Cγ- and TgMEF2Cγ+ mice. (N = 6). Data are presented as mean ±s.e.m. One-way ANOVA (*p< 0.05 vs WT). (For interpretation of the references to color in this figure legend, the reader is referred to the web version of this article.)

+ revealed cardiomyocytes with focal sarcomeric disarrangement (Fig. 5b). Quantitative analysis showed 14% of fragmented sarcomeres in the TgMEF2Cγ+, compared to 0.6% and 1.94% in the WT and TgMEF2Cγ−, respectively (Fig. 5c). No significant changes were detected in the histological or at the ultrastructural level in the hearts of TgMEF2Cγ−.

3.8. Cell cycle, energy metabolism and structural genes are altered in the TgMEF2Cγ+ mice

With the evidence of multiple changes in gene expression induced by MEF2Cγ+ overexpression in neonatal and adult cardiomyocytes, we were interested in examining if similar changes were present in the failing hearts of TgMEF2Cγ+ mice. We performed real-time PCR analysis of representative markers of cell cycle modulators, energy metabolism and cardiomyocyte organization and structure in samples of the hearts of TgMEF2Cγ+ and TgMEF2Cγ− mice. As shown in Fig. 5d−e, there were significant increases in the transcripts of the Ccne1-Cdk2 complex in the LV from the TgMEF2Cγ+ mice. By contrast, Ccne1 transcripts were reduced in the hearts of TgMEF2Cγ− as compared to wild-type mice (Fig. 5d). Moreover, immunohistochemical analysis for the mitosis marker pH3 showed an increased number of pH3-Ser10-positive cardiomyocytes in the hearts of TgMEF2Cγ+ mice, indicating an enhanced mitotic entry in the cardiomyocytes of this lineage (Fig. 5f−g). Quantitative analysis of TUNEL-positive nuclei of cardiomyocytes revealed an increased number of (3-fold) apoptotic cell death in the TgMEF2Cγ+ hearts (Fig. 5h−i). These results support the notion that the transgenic expression of MEF2Cγ+ in the mouse heart induces cardiomyocyte cell

cycle re-entry, without cytokinesis, which culminates in cell death, similarly to the observations in cardiomyocytes in vitro.

The transcripts of genes that were downregulated in NRVMs transduced with MEF2Cγ+ vector were similarly changed in the hearts of TgMEF2Cγ+ mice. Genes involved in energy metabolism, such as Ckm, Ppargc1a, and Ppara (Fig. 5j−m) and cytoskeletal/structural genes such as Myh6 and α-actinin (Actn2) were downregulated in the hearts of the TgMEF2Cγ+ mice (Fig. 5n−o). However, in contrast to what was found in NRVMs transduced with MEF2Cγ-, Ckm, Myh6 and Actn2 were upregulated in MEF2Cγ− transgenic compared to wild-type mice (Fig. 5j, n-o).

Taken together, the cardiac-specific overexpression of MEF2Cγ+ variant induces HF paralleled by partial re-entry in the cell cycle, and downregulation of genes related to energy metabolism and cardiomyocyte structure, which are likely to explain the ensuing structural and functional alterations in the heart of this transgenic mouse model.

3.9. Increased cell cycle markers, reduced energy metabolism and cytoskeletal/structural genes in human and mouse failing hearts

Given the enhanced expression of the MEF2Cγ+ transcripts in human and in mouse failing hearts, we next explored whether there were derangements in the expression of the cell cycle, energy metabolism and structural marker genes in the human and mouse failing hearts. Cell cycle markers such as Ccne1 and Cdk2 were both increased in failing mouse hearts while CDK2 was increased in failing human hearts (Fig. 6a,b). Besides, energy metabolism (human − CKM and PPARGC1B and Mouse - Ckm, Ppara, Ppargc1a) (Fig. 6c,d) and structural
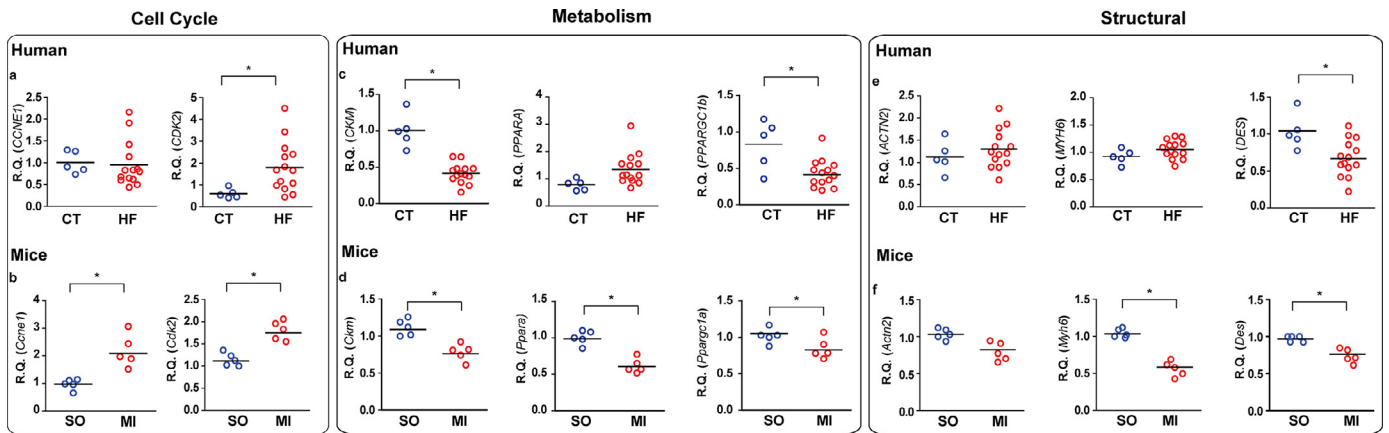
Fig. 6. Increased MEF2Cγ+ correlates to increased cell cycle markers, reduced energy metabolism and structural genes in human and mouse failing hearts; (a, c, e) Real time PCR of cell cycle, metabolism and structural genes in sample of infarcted human hearts. HF: heart failure. CT: Control. (CT N = 5; HF N = 14) Data are presented as mean ±s.e.m. (*$p <$ 0.05 vs CT). (b, d, f) Real time PCR of cell cycle, metabolism and structural genes in sample of mice failing hearts. MI: myocardial infarction. SO: Sham Operated. (N = 5) Data are presented as mean ±s.e.m. Unpaired Student t-test (*$p <$ 0.05 vs SO).

genes (Human − *DES* and Mouse - *Myh6* and *Des*) were downregulated in the failing hearts (Fig. 6e,f). These findings parallel those obtained in isolated NRVMs transduced with the MEF2Cγ+ vector and in the failing heart of the TgMEF2Cγ+ mice, implying that the enhanced expression of the MEF2Cγ+ transcript may be an important factor contributing to the degeneration and death of cardiomyocytes in failing hearts.

4. Discussion

This study provides evidence for a causal relationship between increased cardiac levels of the transcriptional repressor variant MEF2Cγ+ and the development of HF. Our findings in mouse and human heart tissue illustrate an increased expression of MEF2C transcripts containing the transrepressor γ fragment in failing hearts. Mechanistically, our results position the MEF2Cγ+ upstream to pathways that regulate the cell cycle, metabolism and contractile apparatus of differentiated cardiomyocytes. Upregulation of MEF2Cγ+ causes an incomplete cell cycle re-entry, dedifferentiation and apoptosis of cardiomyocytes which underlie the pathological cardiac remodelling and HF in the MEF2Cγ+ transgenic mouse model. Further, our work shows that overexpression of MEF2Cγ+ concurs with downregulation of a set of MEF2 target genes, including genes coding for regulators of the cell cycle, cytoskeletal proteins, contractile apparatus and metabolism. These findings suggest that a widespread downregulation of MEF2 target genes may be the initial event that determines an extensive transcriptional reprogramming and the deleterious alterations induced by MEF2Cγ+ in cardiomyocytes.

Our results demonstrate that increases of the MEF2Cγ+ to the levels seen in murine and human failing hearts are sufficient to cause cardiomyocyte dropout, due to structural disarray and apoptosis. Conceptually, downregulation of genes coding for regulators of energy metabolism, sarcomeric and cytoskeletal proteins, might account for the extensive disarray in cardiomyocyte structural organization and impairment of contractile function, and consequently the development of HF [22−24]. Moreover, our data show that MEF2Cγ+ overexpression induces cardiomyocyte apoptosis both in vitro and in vivo, which besides the impairment of contractile activity, is a critical pathogenic event in the progressive cardiac dysfunction and failure [25,26]. Although many distinct pathways can lead to apoptosis of cardiomyocytes, forcing cardiomyocytes into the cell cycle has been shown in many instances to culminate in apoptosis and lethal HF [27]. More specifically, the incomplete induction of cell cycle can activate the G1/S and G2/M checkpoint signalling in consequence of an accumulation of damaged DNA and failure to complete mitosis, which can lead to cell death [19,20]. Much evidence has accrued that proteins otherwise

associated to the regulation of the cell cycle also participate in mediating cardiomyocyte cell death, including cyclins, cyclin-dependent kinases, CDK inhibitors (p21), Rb Family members, E2Fs and E2F target genes [28]. Consistent with these previous data, our present results show that several genes that drive cell cycle were upregulated in MEF2Cγ+ overexpressing cardiomyocytes. However, none of the genes recognized as direct regulators of the cell cycle seem to be targets of MEF2 transcription factors. Instead, MEF2Cγ+ overexpression was accompanied by an early downregulation of cell cycle inhibitors such as *p15, p16, p19* and *p21*, suggesting that their direct or indirect inhibition by MEF2Cγ+ might contribute to induce the cell cycle re-entry in the cardiomyocytes overexpressing MEF2Cγ+. Thus, we postulate that MEF2Cγ+ promotes loss of cardiomyocyte structural and functional integrity, and ultimately cell death, via direct or indirect deactivation of multiple genes controlled by MEF2 signalling, which results in disassembly of sarcomeric and cytoskeletal organization, profound changes in metabolism and activation of cell cycle associated with a rather extensive transcriptional reprogramming. Furthermore, it is worth noting that the alterations induced by MEF2Cγ+ are akin to partial dedifferentiation of cardiomyocytes, which also recapitulates several phenotypic features seen in cardiomyocytes during pathologic remodelling [29,30].

Inclusion of the alternative γ domain provides for MEF2C repressor isoforms that carry a phosphoserine-dependent transrepressor function [14]. Despite this potentially important implication in MEF2C biology, to our knowledge, the role of the alternative γ fragment in the MEF2C function has not been illustrated before. Our findings that MEF2Cγ+ overexpression results in gene deactivation of many MEF2 target genes of cardiomyocytes are in line with the repressive function of this variant of MEF2C. This repressive effect might be related to a direct interaction of such a variant with the specific MEF2 sites in the regulatory regions of MEF2 target genes, implying a role for the recognition of cis-regulatory regions by the MADS-box/MEF2 DNA binding domain of MEF2Cγ+ in the repression of MEF2-target genes. However, as the transrepressor function of the γ fragment seem to be autonomous [14], the effects of γ fragment are likely to involve the recruitment and physical interaction with transcriptional co-repressors. Besides, data from the present study indicate that the MEF2Cγ+ may work as a dominant-negative abrogating the transactivation activity of MEF2A, MEF2C and MEF2D, an effect that might also contribute to the detrimental effects of MEF2Cγ+ in cardiomyocytes. In support to this view, previous studies have shown that inhibition of MEF2A or MEF2D in cardiomyocytes results in cell-cycle reentry followed by programmed cell death with a significant reduction in sarcomeric genes and upregulation of cell cycle-related

genes [31,32]. Alternatively, as MEF2 by itself is a major regulator of its own promoter activation [33], one might speculate that the MEF2Cγ+ would cause widespread downregulation of gene expression by reducing the expression of the transactivator variants of MEF2C gene. Arguing against this hypothesis, however, are findings that in cardiomyocytes overexpressing MEF2Cγ+ there were no major changes in the expression of MEF2 transcripts.

Here, the sarcomeric genes *Ckm, Myh6 and Actn2* were downregulated in TgMEF2Cγ+ but upregulated in TgMEF2Cγ- mice. These antagonistic effects could be explained by the fact that these genes are transcriptionally regulated by MEF2 factors [34–37]. Consequently, cardiomyocytes overexpressing the γ repressor domain display downregulation of sarcomeric genes and sarcomeric disassembly. Accordingly, previous studies showed that the transcription inhibition of MEF2C by lysine methyltransferase G9a induces downregulation of sarcomeric-related genes and sarcomeric disassembly in muscle cells [38].

An important aspect uncovered by our study is that MEF2Cγ+ variant is increased to a level that can induce cardiomyocyte detrimental effects in the human and mouse failing hearts, implying that this transrepressor variant of MEF2C may play a role in the pathogenesis of HF in general. Based on this, we propose that MEF2C pre-mRNA could be a downstream target of abnormally activated intracellular signalling mechanisms, leading to a preferential synthesis of MEF2Cγ+ variant via the contribution of transacting splicing factors. Several splicing factors have been implicated in the regulation of cardiac function and the regulation of the expression of MEF2 variants. For instance, RBFOX1 is a key transacting RNA splicing regulator in cardiomyocytes during HF [16]. Mechanistically, RBFOX1 has global effects on cardiac mRNA splicing in cardiomyocytes and directly regulates isoform switch from α1 to α2 in splicing variants of the MEF2 family. Interestingly, RBFOX1-mediated MEF2 splicing seems to contribute to cardiomyocyte pathological gene induction. Most remarkably, however, cardiac-specific re-expression of RBFOX1 could significantly attenuate HF in mice. Moreover, other factors such as heterogeneous nuclear ribonucleoprotein U (hnRNP U) and RBM20 are also implicated in the regulation of splicing in cardiomyocytes [39,40] and might be involved in both, the regulation of MEF2 splicing variants and pathogenesis of heart failure.

In summary, we have demonstrated that enhanced expression of the transrepressor MEF2Cγ+ to levels seen in patients with advanced heart failure may induce detrimental alterations in cardiomyocytes and consequently in cardiac pump function. Therefore, the results of this study position the MEF2Cγ+ and the mechanisms that control its expression in the failing heart as potential targets for pharmacological strategies aimed at protecting the heart from progressing into failure.

Funding sources

Declaration of competing interest

The authors declare that they have no conflict of interest.

Acknowledgments

Supplementary materials

Supplementary material associated with this article can be found in the online version at doi:10.1016/j.ebiom.2019.11.032.

References

[1] Mann DL, Bristow MR. Mechanisms and models in heart failure: the biomechanical model and beyond. Circulation 2005;111(21):2837–49.
[2] Dorn 2nd GW. Having a change of heart: reversing the suicidal proclivities of cardiac myocytes. Trans Am Clin Climatol Assoc 2009;120:189–98.
[3] Xie M, Burchfield JS, Hill JA. Pathological ventricular remodeling: therapies: part 2 of 2. Circulation 2013;128(9):1021–30.
[4] van Berlo JH, Maillet M, Molkentin JD. Signaling effectors underlying pathologic growth and remodeling of the heart. J Clin Invest 2013;123(1):37–45.
[5] McKinsey TA, Olson EN. Toward transcriptional therapies for the failing heart: chemical screens to modulate genes. J Clin Invest 2005;115(3):538–46.
[6] Barry SP, Townsend PA. What causes a broken heart−molecular insights into heart failure. Int Rev Cell Mol Biol 2010;284:113–79.
[7] van Oort RJ, van Rooij E, Bourajjaj M, Schimmel J, Jansen MA, van der Nagel R, et al. MEF2 activates a genetic program promoting chamber dilation and contractile dysfunction in calcineurin-induced heart failure. Circulation 2006;114(4):298–308.
[8] Xu J, Gong NL, Bodi I, Aronow BJ, Backx PH, Molkentin JD. Myocyte enhancer factors 2A and 2C induce dilated cardiomyopathy in transgenic mice. J Biol Chem 2006;281(14):9152–62.
[9] Kim Y, Phan D, van Rooij E, Wang DZ, McAnally J, Qi X, et al. The mef2d transcription factor mediates stress-dependent cardiac remodeling in mice. J Clin Invest 2008;118(1):124–32.
[10] Pereira AH, Clemente CF, Cardoso AC, Theizen TH, Rocco SA, Judice CC, et al. MEF2C silencing attenuates load-induced left ventricular hypertrophy by modulating mTOR/S6K pathway in mice. PLoS ONE 2009;4(12):e8472.
[11] Putt ME, Hannenhalli S, Lu Y, Haines P, Chandrupatla HR, Morrisey EE, et al. Evidence for coregulation of myocardial gene expression by MEF2 and nfat in human heart failure. Circ Cardiovasc Genet 2009;2(3):212–9.
[12] Cortes R, Rivera M, Rosello-Lleti E, Martinez-Dolz L, Almenar L, Azorin I, et al. Differences in MEF2 and nfat transcriptional pathways according to human heart failure aetiology. PLoS ONE 2012;7(2):e30915.
[13] Black BL CR. Myocyte enhancer factor 2 transcription factors in heart development and disease editor. In: Rosenthal NHR, editor. Heart development and regeneration. 2. Oxford: Academic Press; 2010. p. 673–99.
[14] Zhu B, Gulick T. Phosphorylation and alternative pre-mRNA splicing converge to regulate myocyte enhancer factor 2C activity. Mol Cell Biol 2004;24(18):8264–75.
[15] Zhu B, Ramachandran B, Gulick T. Alternative pre-mRNA splicing governs expression of a conserved acidic transactivation domain in myocyte enhancer factor 2 factors of striated muscle and brain. J Biol Chem 2005;280(31):28749–60.
[16] Gao C, Ren S, Lee JH, Qiu J, Chapski DJ, Rau CD, et al. RBFox1-mediated rna splicing regulates cardiac hypertrophy and heart failure. J Clin Invest 2016;126(1):195–206.
[17] Ribeiro GA, da Costa CE, Lopes MM, Albuquerque AN, Antoniali F, Reinert GA, et al. Left ventricular reconstruction benefits patients with ischemic cardiomyopathy and non-viable myocardium. Eur J Cardio-Thor Surg 2006;29(2):196–201 Official Journal of the European Association for Cardio-thoracic Surgery.
[18] Dor V, Saab M, Coste P, Kornaszewska M, Montiglio F. Left ventricular aneurysm: a new surgical approach. Thorac Cardiovasc Surg 1989;37(1):11–9.
[19] Wei Y, Yu L, Bowen J, Gorovsky MA, Allis CD. Phosphorylation of histone H3 is required for proper chromosome condensation and segregation. Cell 1999;97(1):99–109.
[20] Zhou J, Ahmad F, Parikh S, Hoffman NE, Rajan S, Verma VK, et al. Loss of adult cardiac myocyte GSK-3 leads to mitotic catastrophe resulting in fatal dilated cardiomyopathy. Circ Res 2016;118(8):1208–22.
[21] Di Giorgio E, Gagliostro E, Clocchiatti A, Brancolini C. The control operated by the cell cycle machinery on MEF2 stability contributes to the downregulation of CDKN1A and entry into S phase. Mol Cell Biol 2015;35(9):1633–47.
[22] Maron BJ, Towbin JA, Thiene G, Antzelevitch C, Corrado D, Arnett D, et al. Contemporary definitions and classification of the cardiomyopathies: an american heart association scientific statement from the council on clinical cardiology, heart failure and transplantation committee; quality of care and outcomes research and functional genomics and translational biology interdisciplinary working groups; and council on epidemiology and prevention. Circulation 2006;113(14):1807–16.
[23] Doenst T, Nguyen TD, Abel ED. Cardiac metabolism in heart failure: implications beyond ATP production. Circ Res 2013;113(6):709–24.
[24] Lichter JG, Carruth E, Mitchell C, Barth AS, Aiba T, Kass DA, et al. Remodeling of the sarcomeric cytoskeleton in cardiac ventricular myocytes during heart failure and after cardiac resynchronization therapy. J Mol Cell Cardiol 2014;72:186–95.
[25] Haunstetter A, Apoptosis IS. basic mechanisms and implications for cardiovascular disease. Circ Res 1998;82(11):1111–29.

[26] Kostin S, Pool L, Elsasser A, Hein S, Drexler HC, Arnon E, et al. Myocytes die by multiple mechanisms in failing human hearts. Circ Res 2003;92(7):715–24.

[27] Agah R, Kirshenbaum LA, Abdellatif M, Truong LD, Chakraborty S, Michael LH, et al. Adenoviral delivery of E2F-1 directs cell cycle reentry and p53-independent apoptosis in postmitotic adult myocardium in vivo. J Clin Invest 1997;100(11):2722–8.

[28] Mercola M, Ruiz-Lozano P, Schneider MD. Cardiac muscle regeneration: lessons from development. Genes Dev 2011;25(4):299–309.

[29] Wang WE, Li L, Xia X, Fu W, Liao Q, Lan C, et al. Dedifferentiation, proliferation, and redifferentiation of adult mammalian cardiomyocytes after ischemic injury. Circulation 2017;136(9):834–48.

[30] Szibor M, Poling J, Warnecke H, Kubin T, Braun T. Remodeling and dedifferentiation of adult cardiomyocytes during disease and regeneration. Cell Mol Life Sci CMLS 2014;71(10):1907–16.

[31] Desjardins CA, Naya FJ. Antagonistic regulation of cell-cycle and differentiation gene programs in neonatal cardiomyocytes by homologous MEF2 transcription factors. J Biol Chem 2017;292(25):10613–29.

[32] Estrella NL, Clark AL, Desjardins CA, Nocco SE, Naya FJ. MEF2D deficiency in neonatal cardiomyocytes triggers cell cycle re-entry and programmed cell death in vitro. J Biol Chem 2015;290(40):24367–80.

[33] Cripps RM, Lovato TL, Olson EN. Positive autoregulation of the myocyte enhancer factor-2 myogenic control gene during somatic muscle development in drosophila. Dev Biol 2004;267(2):536–47.

[34] Molkentin JD, Markham BE. Myocyte-specific enhancer-binding factor (MEF-2) regulates alpha-cardiac myosin heavy chain gene expression in vitro and in vivo. J Biol Chem 1993;268(26):19512–20.

[35] Bour BA, O'Brien MA, Lockwood WL, Goldstein ES, Bodmer R, Taghert PH, et al. Drosophila MEF2, a transcription factor that is essential for myogenesis. Genes Dev 1995;9(6):730–41.

[36] Sandmann T, Jensen LJ, Jakobsen JS, Karzynski MM, Eichenlaub MP, Bork P, et al. A temporal map of transcription factor activity: mef2 directly regulates target genes at all stages of muscle development. Dev Cell 2006;10(6):797–807.

[37] Martin JF, Schwarz JJ, Olson EN. Myocyte enhancer factor (MEF) 2C: a tissue-restricted member of the MEF-2 family of transcription factors. Proc Natl Acad Sci USA 1993;90(11):5282–6.

[38] Ow JR, Palanichamy Kala M, Rao VK, Choi MH, Bharathy N, Taneja R. G9a inhibits mef2c activity to control sarcomere assembly. Sci Rep 2016;6:34163.

[39] Ye J, Beetz N, O'Keeffe S, Tapia JC, Macpherson L, Chen WV, et al. hnRNP u protein is required for normal pre-mRNA splicing and postnatal heart development and function. Proc Natl Acad Sci USA 2015;112(23):E3020–9.

[40] Maatz H, Jens M, Liss M, Schafer S, Heinig M, Kirchner M, et al. RNA-binding protein RBM20 represses splicing to orchestrate cardiac pre-mRNA processing. J Clin Invest 2014;124(8):3419–30.